APEM journal

Advances in Production Engineering & Management
Volume 13 | Number 3 | September 2018 | pp 267–278
https://doi.org/10.14743/apem2018.3.289

ISSN 1854-6250
Journal home: apem-journal.org
Original scientific paper

Design, finite element analysis (FEA), and fabrication of custom titanium alloy cranial implant using electron beam melting additive manufacturing

Ameen, W.[a,b,*], **Al-Ahmari, A.**[a,b], **Mohammed, M.K.**[b], **Abdulhameed, O.**[a,b], **Umer, U.**[b], **Moiduddin, K.**[b]

[a]Industrial Engineering Department, King Saud University, Kingdom of Saudi Arabia
[b]Princess Fatima Alnijiris's Research Chair for Advanced Manufacturing Technology (FARCAMT Chair), Advanced Manufacturing Institute, King Saud University, Kingdom of Saudi Arabia

ABSTRACT

Skull defect reconstruction is one of the most difficult challenges faced by the surgeons because of the complex shape of the skull. Skull defects are dramatically increasing with the increase in road accidents, tumors, and wars, thereby increasing the demand for reconstruction of skull. It is difficult to manufacture standard implants for skull defects especially for large and complex defects, due to the complexity and the difference in anatomy of skulls. Design and fabrication of custom cranial implant is required in these cases. The conventional technologies face multiple challenges in fabricating lightweight custom cranial implants closer to that of bone in terms of weight; the difference in the weight introduces stress-shielding effects onto the surrounding bone. In order to overcome this problem, several researches proposed lattice structure implants fabricated by additive manufacturing. However, lattice structure implants are difficult to remove later when some problems are encountered. This paper presents a methodology of design analysis and fabrication of solid lightweight custom cranial implant using additive manufacturing. A Case study is presented where, a custom cranial implant is designed and analysed using finite element analysis (FEA) and then fabricated using electron beam melting (EBM) additive manufacturing. The titanium alloy Ti6Al4V which is biocompatible and non-toxic is used as the implant material. The functionality, fitting, and aesthetic of the proposed design are evaluated. The results show the successful fabrication of thin custom cranial implant for skull defect reconstruction via EBM technology. The fabricated implant has sufficient strength, weight close to the weight of the removed bone portion while maintaining a good fit and aesthetics.

ARTICLE INFO

Keywords:
Additive manufacturing;
Cranial implant;
Titanium alloy (Ti6Al4V);
Electron beam melting (EBM);
Finite element analysis (FEA)

**Corresponding author:*
wadeaameen@gmail.com
(Ameen, W.)

Article history:
Received 17 July 2018
Revised 13 August 2018
Accepted 24 August 2018

1. Introduction

Skull defect reconstruction is one of the most difficult surgical operations, due to the complexity of the skull shape and the difference of the skulls anatomy. The best way of treating skull defects would be autogenous bone transplantation as this will have less complications of infection, aggressive foreign body reaction, extrusion and damage to the soft tissue and skin [6]. However for the large and complex defects, the use of autologous bone reconstruction is restricted due to the limited availability of donors. Hence, there is a push towards other material implants. Titanium alloy (Ti6Al4V) is biocompatible (non-toxic and not rejected by the body), lightweight and high strength

alloy suitable for applications like medical implants [42, 43]. In general, it is difficult to manufacture standard implants for skull defects as compared to joint prosthesis because of the complexity and the difference in anatomy of the skulls. Therefore, cranial implant are fabricated on a customized and individual basis. Over the years, attempts were made to produce Ti6Al4V implants for large skull defects through manufacturing techniques like Casting, Milling and Forming. These processes invariably suffer from the problems associated with Ti6Al4V. For instance, Machining of Ti6Al4V is very hard and expensive. Casting on the other hand is cost effective but time consuming. Metal-based Additive Manufacturing has shown favorable results in custom built implant fabrication with properties as good as wrought and cast, if not better.

Additive Manufacturing (AM) is one of the latest approaches used for manufacturing products in advanced applications [1]. In AM, parts are fabricated by adding the material in a layer by layers pattern. This is the opposite of machining process, in which the material is removed or subtracted from a block to achieve the shape of the desired object [1]. In general, AM technologies are used to produce parts for high performance applications within biomedical, aerospace and automotive industries. The primary function of these technologies is to produce complicated internal features with functional design where machining and casting would require too much of lead-time, and wastage of material [2]. Medical applications generally involve complex parts and customization. In recent years AM technologies have been successfully utilized to produce various custom implants [3, 43]. Electron Beam Melting (EBM) is one of the latest AM technologies suitable for bio-medical applications [43]. In this process an electron beam melts the metal alloy powder into near net shape solid part in a layer by layer manner under controlled vacuum [4, 5].

In this research, EBM system commercialized by ARCAM AB is used to fabricate a lightweight cranial implant from Ti6Al4V ELI alloy. The fabricated implant delivers the functionality, geometric fit and aesthetics for skull defect reconstruction.

2. Literature review

Medical implants are commonly used for bone reconstructions in orthopedic, cranio-maxillofacial, dental and cosmetic surgery. The custom implant is designed and fabricated to fit the specification of patient. Design of cranial implants is the first step in skull defect reconstruction. The geometry of the implant is gathered from Computerized Tomographic (CT) scan data to achieve the fit. The design is further modified to achieve desired mechanical properties for improved performance of the implant. He *et al.* have presented a methodology in custom designed implant with the integration of Magnetic Resonance Imaging (MRI) scanning, image processing and AM technology [7]. Selection of implants materials is critical issue in craniofacial reconstructions. Alaa Kamel Abdel-Haleem *et al*. have described the advantages and disadvantages of using the rib grafts in skull and neck reconstruction [6]. Several biocompatible materials such as polyethylmethacrylate (PMMA), hydroxyapatite (HA) and Polyethylene were earlier used as the implant materials but each one of those has their own limitations [8-10].

Titanium alloy (Ti6Al4V ELI) is used in various alloys of iron, vanadium, aluminum, etc. [11]. It is used especially in aerospace, military and increasingly more in medical prosthetics [12]. Titanium alloys are one of the most widely used biocompatible material when compared to other bio-metals such as stainless steel and cobalt-chromium [13]. Ti6Al4V ELI (extra low interstitial) is the highest purity version of Ti6Al4V. It is commonly used in maxillofacial and craniofacial regions. Typically Titanium implants are fabricated as solid or mesh forms [14]. Several technologies have been used for fabrication the cranial implants. Traditionally the medical sculptors were employed to manufacture the implant based on the anatomical model using wax and clay [15]. Currently, however anatomical shape reconstructions are done using clay and computer aided design tools. Since the latter half of 1990's, Computer aided design cranial implants has been developed [16, 17]. Also a Computer Numerically Controlled (CNC) milling machine [18], direct milling method [19], and casting method are used for the fabrication of cranial implants [20].

In earlier studies, cranial defects were repaired using bulk titanium implants, which were 1.6 times more heavier than the removed bone [21, 29]. This bulky titanium implant due to the differences in young's modulus introduces stresses on the surrounding bone-implant interface known as

stress-shielding effect [22]. Researchers have tried to reduce the stress shielding effect, by introducing porous structure and making it lighter in weight, but with no clear evidence and investigation on mechanical and structural properties[23, 24]. In addition, the porous structure are difficult to remove later in case of some problem. Recently additive-manufacturing technology has shown potential for producing custom medical implants with altered mechanical properties to match the requirements of bone replacements. EBM technology has been successfully employed in the fabrication of titanium based custom design implants in orthopedic, craniofacial and maxillofacial surgeries [25-28]. This paper presents a methodology in the design, analysis and fabrication of a thin and lighter customized cranial implant with mechanical properties closer to that of bone using additive manufacturing.

3. Materials and methods

3.1 Design of the cranial defect implant

The computed tomography (CT) scan data of the patient as a Digital Imaging and Communica-tions in Medicine (DICOM) file is acquired. The CT data is then processed using MIMICS® software to generate the CAD model for the required anatomy.

Fig. 1 shows the screenshot of the MIMICS® with scan data in three orientations: axial, sagittal and coronal with a space to display the reconstructed 3D image. Segmentation of CT 2D slice images is done by selecting specific image intensities (Hounsfield units) within the region of interest. Hounsfield units (HU) is a system to measure the attenuation coefficient of tissues in CT scan images. HU are also termed CT numbers. The use of CT numbers or Hounsfield units provides an indication of the nature of the tissues. Specific tissues such as bone, skin and muscles are identified by their Hounsfield units.

Thresholding is then carried out by selecting the upper and lower threshold values of image intensities. Similarly, the pathological area is also delineated. Bone has a higher Hounsfield value when compared to skin and soft tissues as it absorbs most of the radiation.

Table 1 shows the Hounsfield values of some tissues that are commonly studied with CT images.

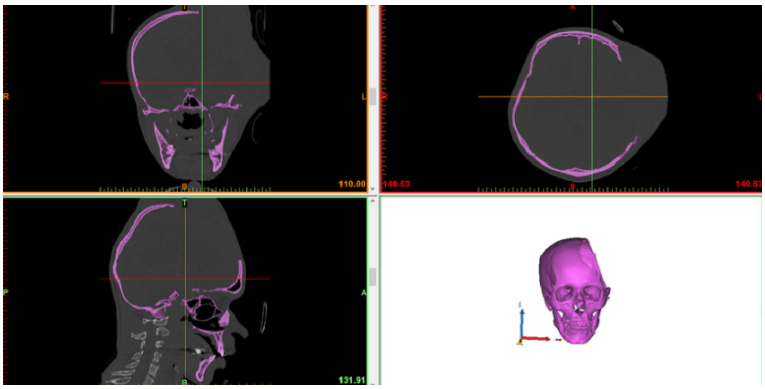

Fig. 1 CT scan images in three orientations

Table 1 Hounsfield values of tissues

Tissue	CT number (HU)
Bone	1000
Liver	40-60
White matter (brain)	46
Grey matter (brain)	43
Blood	40
Muscle	Oct-40
Kidney	30
Cerebrospinal fluid	15
Water	0
Fat	50 to -100
Air	-100

Region growing is the process by which noise is minimized and structures that are not connected in the image data are eliminated, resulting in a set of pixels that are connected within the same layer as well as with the upper and lower layers of data as seen in Fig. 2(a). By using the 3D reconstruction function, a 3D rendered model of the anatomy is generated. A skull with the defect rendered is seen Fig. 2(b). The reconstructed skull defect model was then used for implant reconstruction using 3 MATIC® software (Materialise NV, Leuven, Belgium). The steps involved during implant reconstruction include creation of a datum plane (symmetry plane) as shown in Fig. 2(c). Assuming the human body structure to be symmetric, the defect side (left) was removed from the center using the datum plane and the right side (healthy) is mirrored to reconstruct the defective area as shown in Fig. 2(d,e,f) respectively. Furthermore, the symmetry skull and the reconstructed skull with defect were merged together as shown in Fig. 2(g). The Boolean subtraction of merged symmetry skull from reconstructed skull with defect is carried out as shown in Fig. 2(h). The cranial implant produced from the subtraction process is shown in Fig. 2(i). Dimension Elite 3d printer is used to fabricate the skull and the implant prototypes as shown in Fig. 2(j,k). The fitness of the designed implant was tested visually as shown in Fig. 2(l) the result show good fitness between the fabricated model and the implant.

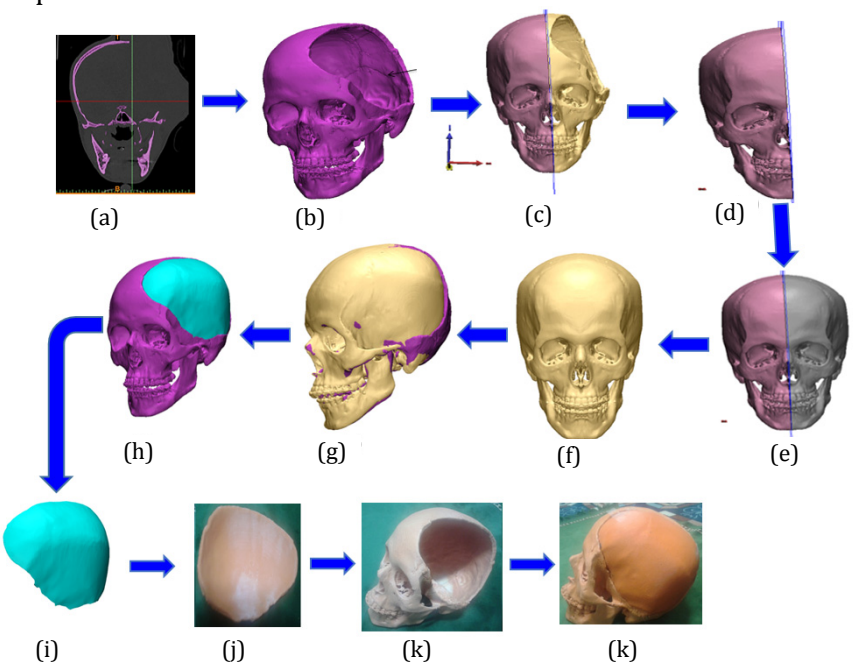

Fig. 2 Design steps of custom cranial defect implant in 3 MATIC®

Four fixation plates were designed with screw hole slots for the fixation and attachment of the screws to the cranium as illustrated in Fig. 3. The designed implant was of the same thicknesses as that of the bone portion 3.18-5.76 mm. In order to minimize the stress shielding effect, the implant thickness was reduced to bring down the weight of the Ti6Al4V ELI implant close to the bone portion of skull. The implant thickness was reduce to 0.5 mm (minimum thickness that can be produced by EBM technology) [30], by an inward offset operation on the thick cranial implant using Geomagic software.

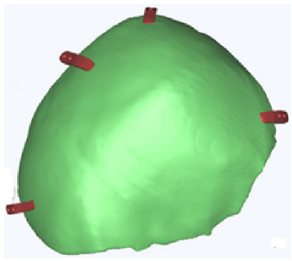

Fig. 3 Cranial implant with fixation lips

3.2 Finite element analysis

Finite element analysis (FEA) method was used to evaluate the functionality of the designed custom cranial implant. Abaqus software was used for pre- processing, solving and post-processing of the models. Table 2 shows the material properties assigned to the FE models, in which cortical bone was assigned to the skull with defect model and Arcam Ti–6Al–4V ELI was assigned to the custom cranial implant [31]. Good quality meshing with Tetrahedron elements was performed on the skull and skull implant model as shown in Fig. 4. Fine mesh was considered for the cranial implant and course mesh for the defected skull model. Table 3 shows the number of elements and nodes used during mesh generation.

Table 2 Material properties used in FE model

Material	Young's modulus (MPa)	Poisson's ratio	Yield strength (MPa)
Cortical bone	13,700	0.3	122
Arcam Ti–6Al–4V ELI	120,000	0.3	930

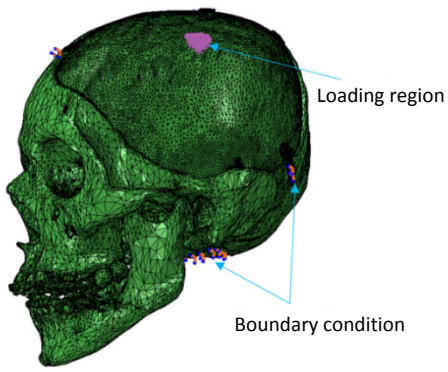

Fig. 4 Mesh generation, loads and boundary condition

A static force was applied in the small circular region (1 cm^2) at the center of the implant. As recommended by the doctors the static loading simulated a relaxed person resting on a pillow. The applied force is 50 N, which corresponds to the approximate weight of the head. In addition, a further forces load of 1780N was applied which simulates the impact of a tennis ball at an average speed of 30 m/s [32-36].

Table 3 Mesh data for both skull and implant

FE Model	Number of elements	Number of nodes
Skull model	179409	368448
Implant model	117252	234532

4. Results and discussion

4.1 Finite element results

Fig. 5 shows the result of static finite element analysis with the application of 50 N force load. The maximum developed stress on the Ti6Al4V ELI implant is 1 MPa which is well below the allowable limit of material. Moreover, it is concentrated on the fixing plates of the implant. The results shows the highest strain and displacement developed on the cranial implant are 0.0000041 mm and 0.00019 mm as shown in Fig. 5(b) and Fig. 5(c), respectively. Maximum strain and displacement is also within allowable limit of material and the maximum strain is concentrated in the fixing plates and the maximum displacement is located in the middle of the implant.

The results of FE model simulating the impact of a tennis ball is shown in Fig. 6. The results shown that the maximum stress, strain and displacement are 36 MPa, 0.00014 mm and 0.0069 mm respectively. In addition, the maximum developed stress and strain is located near the fixing plates whereas the displacement is found in the middle of the implant.

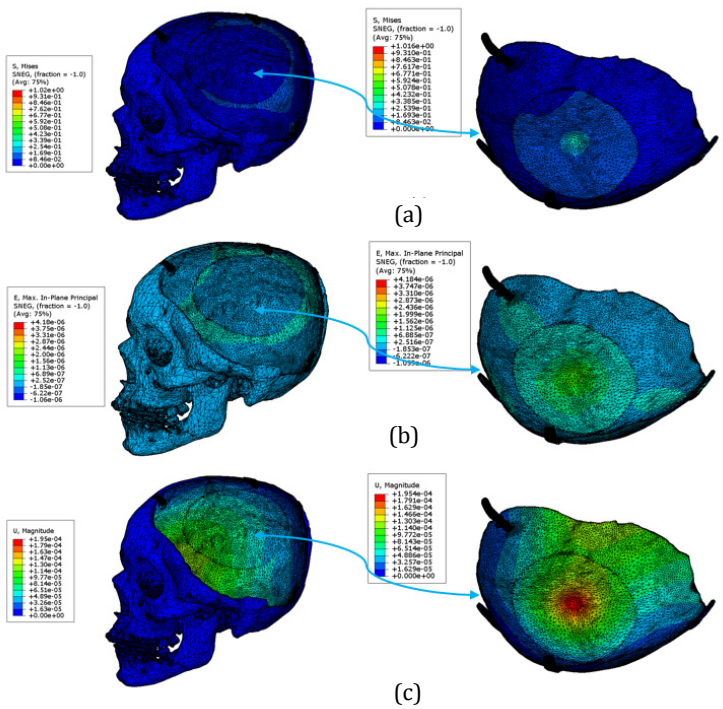

Fig. 5 Results of static loading: (a) Stress distribution, (b) Resulting strain, (c) Maximum displacement

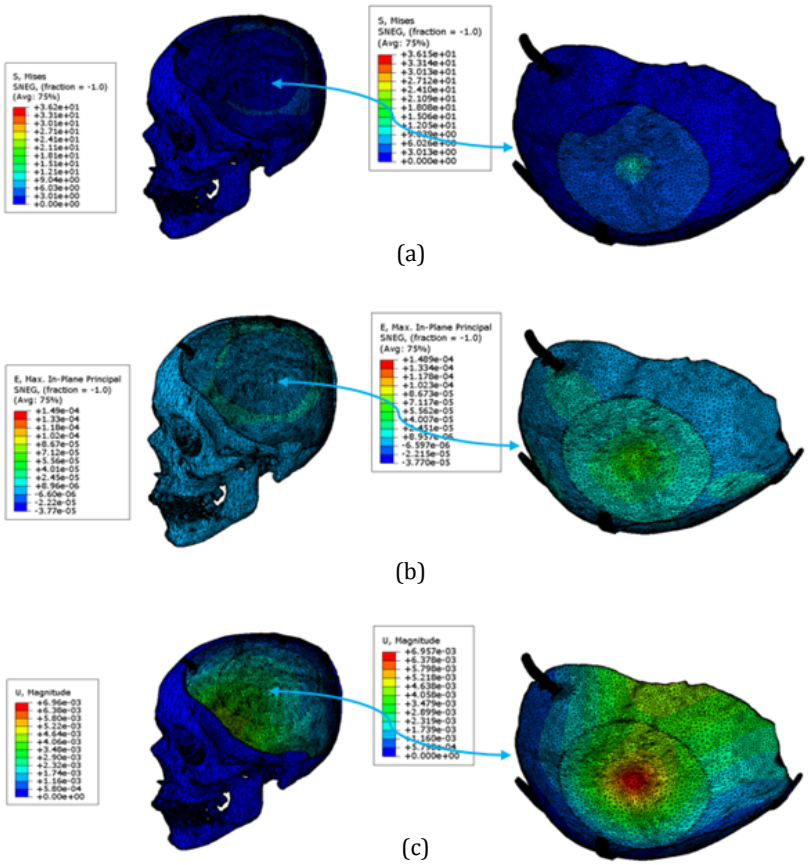

Fig. 6 Results of impact loading: (a) Stress distribution, (b) Resulting strain, (c) Maximum displacement

The results of both test loading showed that the maximum stresses, strains and displacements were within allowable limit of the Ti6Al4V ELI material, validating the designed implant with 0.5 mm thickness to be able to withstand load.

4.2 Implant fabrication results

Titanium alloy (Ti6Al4V) powder with the chemical compositions as shown in Table 4 is used as the feedstock material. The particle size analysis revealed that the size of powder particles in the range 53-107 μm with mean approximation of 75 μm as shown in Fig. 7. The morphology of the powder particles are mostly spherical in shape with little deviations in geometry. Fig. 8 illustrates the Scanning electron microscope (SEM) analysis of Ti6Al4V ELI powder using JSM-6610LV (JOEL, United States).

Table 4 Chemical composition of the Ti6Al4V ELI powder

Element	Al	V	C	Fe	O	Ti
Weight %	6.04	4.05	0.013	0.0107	0.13	Bal.

ARCAM A2 EBM machine was used to fabricate the custom Ti6Al4V ELI implant. The schematic of EBM and the Arcam setup used in this work is shown in Fig. 9 and 10, respectively [40]. EBM setup comprises of a heated tungsten filament (cathode) in a grid cup (anode) which produces the electron beam. The electrons are charged and accelerated to a kinetic energy of about 60 keV producing a maximum power of 4.8 kW with a beam spot size of 0.1-0.4 mm.

The three magnetic lenses including astigmatism lens, focus lens and deflection coils controls the direction of electron beam. The two hoppers holds the feedstock powder and the raking blade is used to spread the powder evenly over the build area. The build table moves down by one layer thickness (50 μm) and a new layer of powder is dispensed as the build progresses. Based on the set layer thickness the electron beam melts the powder in a layer by layer manner to produce the desired geometry [37,38]. The total built time for the cranial implant was approximately 8 hours with additional 3 to 4 hours for in cooling and 1 hours for post-processing (removing the sintered powder and support structures).

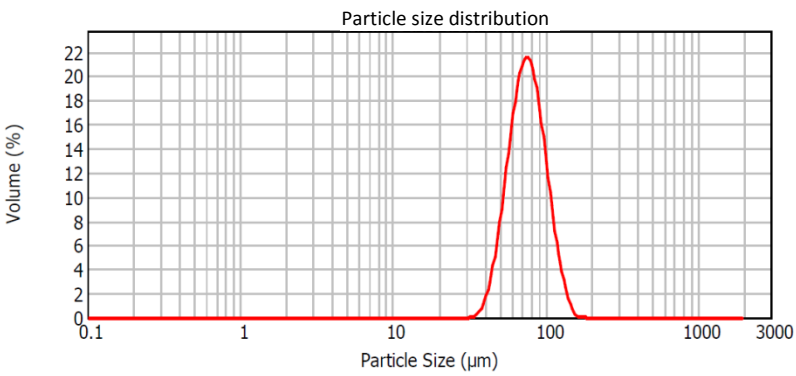

Fig. 7 Powder particle size distribution measured by laser diffraction technique

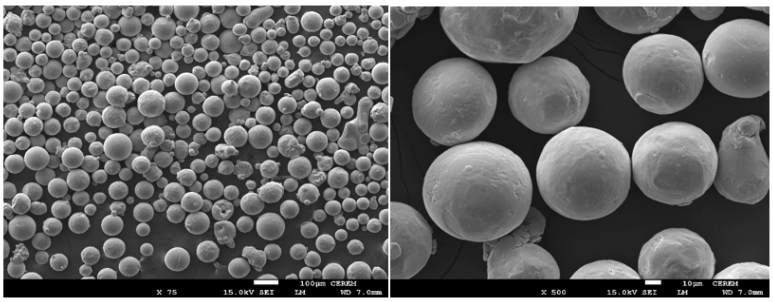

Fig. 8 Scanning electron microscope image of Ti6Al4V ELI powder particles

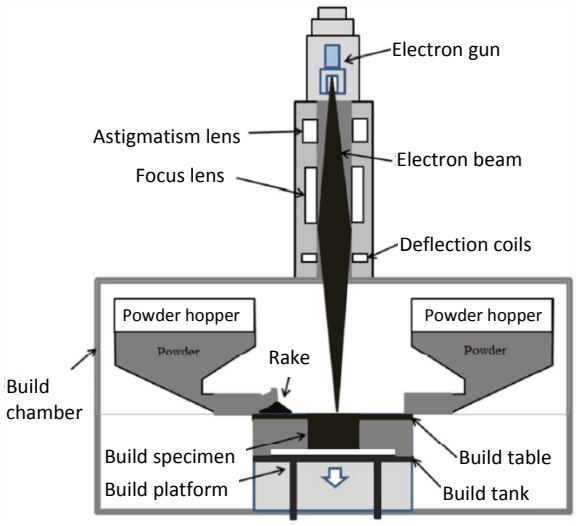

Fig. 9 Schematic of EBM process

Fig. 10 EBM setup from ARCAM

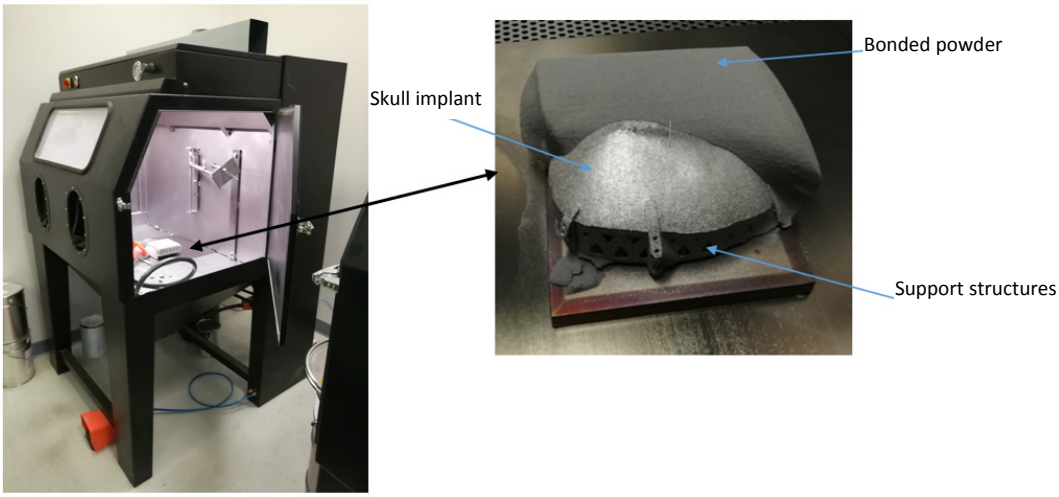

Fig. 11 Powder recovery system

The entire built process takes place under high vacuum of 0.1 Pa to 0.001 Pa. After the completion of built, fabricated parts are cooled down to room temperature under helium environment to prevent oxidation. The build envelope with fabricated custom implant is then taken to the powder recovery system (PRS) to blast the sintered powder using compressed air as shown in Fig. 11.

The support structures are then removed and the thickness of the implant is measured using the screw gauge. The thickness was found to be approximately 0.52 mm as shown in Fig. 12.

The weight of the fabricated implant is measured using digital weighing machine. The weight was found to be close to the weight of the bone portion that was removed from the skull, assuming the bone density to be ρ =210 kg m−3 [39]. The details of the fabricated implant and the equivalent bone portion are listed in Table 5.

To evaluate the accuracy of the fabricated implant, it is first scanned using ViuScan hand scanner as show in Fig. 13. Then Geomagic Qualify software is used for the 3D comparison. The Geomagic quality is one of the commonly used techniques to graphically represent the surface deviation between two models.

The EBM fabricated cranial implant was taken as test model and the original CT scan was taken as reference model. Using this software, the scanned EBM fabricated model was superimposed onto the reference CAD model with the Best Fit Alignment function using 1500 points. The differences were analyzed as positive and negative deviations. A positive deviation occurs if the test (scanned) model is larger than the reference (Original CT scan) model and a negative deviation if it is smaller.

The mean deviations and root mean square of the deviations (RMSD) between test and reference model were calculated [41]. In order to demonstrate the magnitude, location and direction of the discrepancies between them, a color coded model was developed as shown in Fig. 14.

(a) (b)

Fig. 12 (a) The fabricated implant with support structure, (b) Implant after the removal of support

Table 5 Weight details of the fabricated and the equivalent bone portion

Material	Thickness (mm)	Volume (mm^3)	Weight (g)
Bone portion	Varying thickness: 3.18-5.76 mm	149114.285	31.314
Ti6Al4V ELI implant	0.52	9758.140	41.574

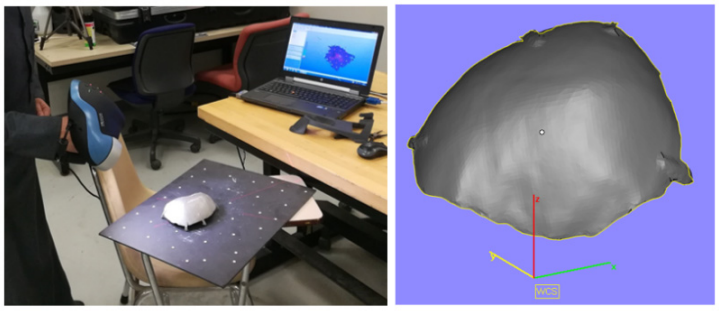

(a) (b)

Fig. 13 (a) Implant scanning, (b) Scanned implant model

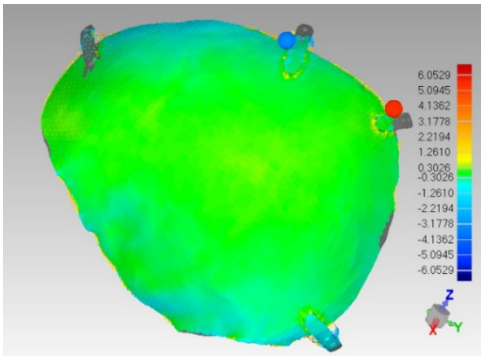

Fig. 14 The 3D comparison result

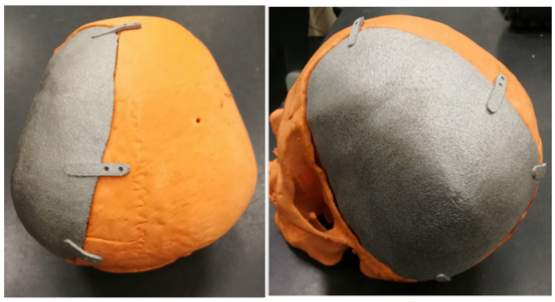

(a) (b)

(c)

Fig. 15 Fabricated custom implant: (a) Top view, (b) Side view, (c) Front view

The results showed that the average positive and negative deviations are 0.321 mm and -0.3515 mm respectively with standard deviation 0.3246 mm and the RMSD deviation is 0.5380 mm. The fit of the fabricated implant was evaluated by fixing it on the 3D printed plastic skull model as shown in Fig. 15. The visual inspection from all the sides shows that fabricated implant successfully achieved a good fit and aesthetics.

5. Conclusion

In this study, a thin solid light weight custom cranial implant is designed, analyzed and fabricated using EBM. The craniofacial implant was designed based upon the patient CT scan images using MIMICS® and 3-MATIC®. Finite element analysis was carried out in order to assess the quality of the developed implant design under different loading conditions. The Ti6Al4V ELI implant of 0.5 mm thickness was then fabricated using EBM technology. The fitness of the fabricated implant was tested on the plastic prototype of the skull. The results showed the successful fabrication of 0.5 mm thick custom cranial implant for skull defect reconstruction via EBM technology while maintaining the structural strength requirements for reconstruction of skull defect . The main advantage of this approach for the skull defect reconstruction is the customizability, flexibility and less lead time for implant fabrication. However, this technology is still expensive and require significant amount of validation and testing before the implant is finally used for reconstruction of the defect.

Acknowledgements

The authors are grateful to the Deanship of Scientific Research, king Saud University for funding through Vice Deanship of Scientific Research Chairs.

References

[1] Gibson, I., Rosen, D.W., Stucker, B. (2010). *Additive manufacturing technologies: Rapid prototyping to direct digital manufacturing,* Springer, New York, USA, doi: 10.1007/978-1-4419-1120-9.

[2] Morgan, L., Lindhe, U., Harrysson, O. (2003). Rapid manufacturing with electron beam melting (EBM) – A manufacturing revolution?, In: *Proceedings of Annual International Solid Freeform Fabrication Symposium – An Additive Manufacturing Conference,* Austin, Texas, USA, 433-438.

[3] Berce, P., Chezan, H., Balc, N. (2005). The application of rapid prototyping technologies for manufacturing the custom implants, In: *Proceedings of 8th ESAFORM Conference on Material Forming,* Cluj-Napoca, Romania, 27-29.

[4] Christensen, A., Kircher, R., Lippincott, A. (2008). Qualification of electron beam melted (EBM) Ti6Al4V-ELI for orthopaedic applications, In: *Proceedings of MPMD, Materials and Processes for Medical Devices Conference,* Palm Desert, USA, 48-53.

[5] Li, X., Wang, C., Zhang, W., Li, Y. (2009). Fabrication and characterization of porous Ti6Al4V parts for biomedical applications using electron beam melting process, *Materials Letters,* Vol. 63, No. 3-4, 403-405, doi: 10.1016/j.matlet.2008.10.065.

[6] Abdel-Haleem, A.K., Nouby, R., Taghian, M. (2011). The use of the rib grafts in head and neck reconstruction, *Egyptian Journal of Ear, Nose, Throat and Allied Sciences,* Vol. 12, No. 2, 89-98, doi: 10.1016/j.ejenta.2011.08.004.

[7] He, Y., Ye, M., Wang, C. (2006). A method in the design and fabrication of exact-fit customized implant based on sectional medical images and rapid prototyping technology, *The International Journal of Advanced Manufacturing Technology*, Vol. 28, No. 5-6, 504-508, doi: 10.1007/s00170-004-2406-y.

[8] Durham, S.R., McComb, J.G., Levy, M.L. (2003). Correction of large (> 25 cm^2) cranial defects with "reinforced" hydroxyapatite cement: Technique and complications, *Neurosurgery,* Vol. 52, No. 4, 842-845, doi: 10.1227/01.NEU.0000054220.01290.8E.

[9] Ducic, Y. (2002). Titanium mesh and hydroxyapatite cement cranioplasty: A report of 20 cases, *Journal of oral and maxillofacial surgery,* Vol. 60, No. 3, 272-276, doi: 10.1053/joms.2002.30575.

[10] Engstrand, T., Kihlström, L., Lundgren, K., Trobos, M., Engqvist, H., Thomsen, P. (2015). Bioceramic implant induces bone healing of cranial defects, *Plastic and Reconstructive Surgery – Global Open,* Vol. 3, No. 8, doi: 10.1097/GOX.0000000000000467.

[11] Charnley, G., Judet, T., Pirou, P., Garreau de Loubresse, C. (2000). Titanium femoral component fixation and experience with a cemented titanium prosthesis, In: Learmonth, I.D. (ed.), *Interfaces in total hip arthroplasty*, Springer, London, UK, 3-10, doi: 10.1007/978-1-4471-0477-3_1.

[12] Moiduddin, K., Darwish, S., Al-Ahmari, A., ElWatidy, S., Mohammad, A., Ameen, W. (2017). Structural and mechanical characterization of custom design cranial implant created using additive manufacturing, *Electronic Journal of Biotechnology,* Vol. 29, 22-31, doi: 10.1016/j.ejbt.2017.06.005.

[13] Niinomi, M. (2008). Mechanical biocompatibilities of titanium alloys for biomedical applications, *Journal of the Mechanical Behavior of Biomedical Materials,* Vol. 1, No. 1, 30-42, doi: 10.1016/j.jmbbm.2007.07.001.
[14] Schipper, J., Ridder, G.J., Spetzger, U., Teszler, C.B., Fradis, M., Maier, W. (2004). Individual prefabricated titanium implants and titanium mesh in skull base reconstructive surgery. A report of cases, *European Archives of Oto-Rhino-Laryngology and Head & Neck,* Vol. 261, No. 5, 282-290, doi: 10.1007/s00405-003-0686-8.
[15] Mazzoli, A., Germani, M., Raffaeli, R. (2009). Direct fabrication through electron beam melting technology of custom cranial implants designed in a PHANToM-based haptic environment, *Materials & Design,* Vol. 30, No. 8, 3186-3192, doi: 10.1016/j.matdes.2008.11.013.
[16] Goyal, S., Goyal, M. K. (2014). Restoration of large cranial defect for cranioplasty with alloplastic cranial implant material: A case report, *The Journal of Indian Prosthodontic Society,* Vol. 14, No. 2, 191-194, doi: 10.1007/s13191-012-0185-y.
[17] Lieger, O., Richards, R., Liu, M., Lloyd, T. (2010). Computer-assisted design and manufacture of implants in the late reconstruction of extensive orbital fractures, *Archives of Facial Plastic Surgery,* Vol. 12, No. 3, 186-191, doi: 10.1001/archfacial.2010.26.
[18] Joffe, J.M., Nicoll, S.R., Richards, R., Linney, A.D., Harris, M. (1999). Validation of computer-assisted manufacture of titanium plates for cranioplasty, *International Journal of Oral and Maxillofacial Surgery,* Vol. 28, No. 4, 309-313, doi: 10.1016/S0901-5027(99)80165-9.
[19] da Costa, D.D., Pedrini, H., Bazan, O. (2009). Direct milling of polymethylmethacrylate for cranioplasty applications, *The International Journal of Advanced Manufacturing Technology,* Vol. 45, No. 3-4, 318-325, doi: 10.1007/s00170-009-1978-y.
[20] da Costa, D.D., Lajarin, S.F. (2012). Comparison of cranioplasty implants produced by machining and by casting in a gypsum mold, *The International Journal of Advanced Manufacturing Technology*, Vol. 58, No. 1-4, 1-8, doi: 10.1007/s00170-011-3388-1.
[21] Saldarriaga, J.F.I., Vélez, S.C., Posada, M.D.A.C., Henao, I.E.B.B., Valencia, M.E.C.A.T. (2011). Design and manufacturing of a custom skull implant, *American Journal of Engineering and Applied Sciences,* Vol. 4, No. 1, 169-174, doi: 10.3844/ajeassp.2011.169.174.
[22] Dujovne, A.R., Bobyn, J.D., Krygier, J.J., Miller, J.E., Brooks, C.E. (1993). Mechanical compatibility of noncemented hip prostheses with the human femur, *The Journal of Arthroplasty,* Vol. 8, No. 1, 7-22, doi: 10.1016/S0883-5403(06)80102-6.
[23] Parthasarathy, J. (2014). 3D modeling, custom implants and its future perspectives in craniofacial surgery, *Annals of Maxillofacial Surgery,* Vol. 4, No. 1, 9-18, doi: 10.4103/2231-0746.133065.
[24] Cho, H.R., Roh, T.S., Shim, K.W., Kim, Y.O., Lew, D.H., Yun, I.S. (2015). Skull reconstruction with custom made three-dimensional titanium implant, *Archives of Craniofacial Surgery,* Vol. 16, No. 1, 11-16, doi: 10.7181/acfs.2015.16.1.11.
[25] Murr, L.E., Gaytan, S.M., Martinez, E., Medina, F., Wicker, R.B. (2012). Next generation orthopaedic implants by additive manufacturing using electron beam melting, *International Journal of Biomaterials,* Vol. 2012, doi: 10.1155/2012/245727.
[26] Al-Ahmari, A., Nasr, E.A., Moiduddin, K., Alkindi, M., Kamrani, A. (2015). Patient specific mandibular implant for maxillofacial surgery using additive manufacturing, In: *Proceedings of 2015 International Conference on Industrial Engineering and Operations Management (IEOM),* Dubai, UAE, 1-7, doi: 10.1109/IEOM.2015.7093788.
[27] Mazzoli, A., Germani, M., Raffaeli, R. (2009). Direct fabrication through electron beam melting technology of custom cranial implants designed in a PHANToM-based haptic environment, *Materials & Design,* Vol. 30, No. 8, 3186-3192, doi: 10.1016/j.matdes.2008.11.013.
[28] Li, X., Wang, C., Zhang, W., Li, Y. (2009). Fabrication and characterization of porous Ti6Al4V parts for biomedical applications using electron beam melting process, *Materials Letters,* Vol. 63, No. 3-4, 403-405, doi: 10.1016/j.matlet.2008.10.065.
[29] Saldarriaga, J.F.I., Vélez, S.C., Posada, M.D.A.C., Henao, I.E.B.B., Valencia, M.E.C.A.T. (2011). Design and manufacturing of a custom skull implant, *American Journal of Engineering and Applied Sciences,* Vol. 4, No. 1, 169-174, doi: 10.3844/ajeassp.2011.169.174.
[30] Syam, W.P., Al-Shehri, H.A., Al-Ahmari, A.M., Al-Wazzan, K.A., Mannan, M.A. (2012). Preliminary fabrication of thin-wall structure of Ti6Al4V for dental restoration by electron beam melting, *Rapid Prototyping Journal,* Vol. 18, No. 3, 230-240, doi: 10.1108/13552541211218180.
[31] Al-Ahmari, A., Nasr, E.A., Moiduddin, K., Anwar, S., Al Kindi, M., Kamrani, A. (2015). A comparative study on the customized design of mandibular reconstruction plates using finite element method, *Advances in Mechanical Engineering,* Vol. 7, No. 7, doi: 10.1177/1687814015593890.
[32] Tsouknidas, A., Maropoulos, S., Savvakis, S., Michailidis, N. (2011). FEM assisted evaluation of PMMA and Ti6Al4V as materials for cranioplasty resulting mechanical behaviour and the neurocranial protection, *Bio-Medical Materials and Engineering,* Vol. 21, No. 3, 139-147, doi: 10.3233/BME-2011-0663.
[33] Allen, T., Goodwill, S., Haake, S. (2008). Experimental validation of a tennis ball finite-element model for different temperatures, In: Estivalet, M., Brisson, P. (eds.), *The Engineering of Sport 7*, Springer Nature, Switzerland, 125-133, doi: 10.1007/978-2-287-09411-8_15.
[34] Chamrad, J., Marcián, P., Borák, L., Wolff, J. (2016). Finite element analysis of cranial implant, In*: Proceedings of 32nd conference with international participation computational mechanics*, Železná Ruda, Czech Republic, doi: 10.13140/RG.2.2.19870.13124.
[35] Parle, D., Ambulgekar, A., Gaikwad, K. (2015). Patient specific design and validation of cranial implants using FEA, In: *Altair Technology Conference,* Bengaluru, India, 1-9.

[36] Ridwan-Pramana, A., Marcián, P., Borák, L., Narra, N., Forouzanfar, T., Wolff, J. (2017). Finite element analysis of 6 large PMMA skull reconstructions: A multi-criteria evaluation approach, *Plos One,* Vol. 12, No. 6, doi: 10.1371/journal.pone.0179325.
[37] Koike, M., Martinez, K., Guo, L., Chahine, G., Kovacevic, R., Okabe, T. (2011). Evaluation of titanium alloy fabricated using electron beam melting system for dental applications, *Journal of Materials Processing Technology*, Vol. 211, No. 8, 1400-1408, doi: 10.1016/j.jmatprotec.2011.03.013.
[38] Karlsson, J. (2015*). Optimization of electron beam melting for production of small components in biocompatible titanium grades,* Doctoral thesis, Acta universitatis upsaliensis.
[39] Margulies, S.S., Thibault, K.L. (2000). Infant skull and suture properties: Measurements and implications for mechanisms of pediatric brain injury, *Journal of Biomechanical Engineering*, Vol. 122, No. 4, 364-371, doi: 10.1115/1.1287160.
[40] Ameen, W., Al-Ahmari, A., Mohammed, M.K., Mian, S.H. (2018). Manufacturability of overhanging holes using electron beam melting, *Metals,* Vol. 8, No. 6, 1-24, doi: 10.3390/met8060397.
[41] Al-Ekrish, A.A., Alfadda, S.A., Ameen, W., Hörmann, R., Puelacher, W., Widmann, G. (2018). Accuracy of computer-aided design models of the jaws produced using ultra-low MDCT doses and ASIR and MBIR, *International Journal of Computer Assisted Radiology and Surgery,* 1-8, doi: 10.1007/s11548-018-1809-4.
[42] Čolić, K., Sedmak, A., Legweel, K., Milošević, M., Mitrović, N., Mišković, Ž., Hloch, S. (2017). Experimental and numerical research of mechanical behaviour of titanium alloy hip implant, *Tehnički vjesnik – Technical Gazette,* Vol. 24, No. 3, 709-713, doi: 10.17559/TV-20160219132016.
[43] Ramakrishnaiah, R., Al Kheraif, A.A., Mohammad, A., Divakar, D.D., Kotha, S.B., Celur, S.L., Hashem, M.I., Vallittu, P.K., Rehman, I.U. (2017). Preliminary fabrication and characterization of electron beam melted Ti-6Al-4V customized dental implant, *Saudi Journal of Biological Sciences,* Vol. 24, No. 4, 787-796, doi: 10.1016/j.sjbs.2016.05.001.